Cell shape–dependent rectification of surface receptor transport in a sinusoidal electric field

Raphael C. Lee,* T. R. Gowrishankar,* Russel M. Basch,* Pravin-Kumar K. Patel,* and David E. Golan‡

*The Biomechanics Section, Department of Organismal Biology & Anatomy, and Plastic Surgery Research Laboratories, Department of Surgery, The University of Chicago, Chicago, Illinois 60637; and ‡Departments of Biological Chemistry and Molecular Pharmacology and of Medicine, Harvard Medical School, and The Hematology/Oncology Division, Brigham and Women's Hospital, Boston, Massachusetts 02115 USA

ABSTRACT In the presence of an extracellular electric field, transport dynamics of cell surface receptors represent a balance between electromigration and mutual diffusion. Because mutual diffusion is highly dependent on surface geometry, certain asymmetrical cell shapes effectively create an anisotropic resistance to receptor electromigration. If the resistance to receptor transport along a single axis is anisotropic, then an applied sinusoidal electric field will drive a net time-average receptor displacement, effectively rectifying receptor transport. To quantify the importance of this effect, a finite difference mathematical model was formulated and used to describe charged receptor transport in the plane of a plasma membrane. Representative values for receptor electromigration mobility and diffusivity were used. Model responses were examined for low frequency (10^{-4}–10 Hz) 10-V/cm fields and compared with experimental measurements of receptor back-diffusion in human fibroblasts. It was found that receptor transport rectification behaved as a low-pass filter; at the tapered ends of cells, sinusoidal electric fields in the 10^{-3} Hz frequency range caused a time-averaged accumulation of receptors as great as 2.5 times the initial uniform concentration. The extent of effective rectification of receptor transport was dependent on the rate of geometrical taper. Model studies also demonstrated that receptor crowding could alter transmembrane potential by an order of magnitude more than the transmembrane potential directly induced by the field. These studies suggest that cell shape is important in governing interactions between alternating current (ac) electric fields and cell surface receptors.

GLOSSARY

μ	electromigration mobility
D	lateral diffusion coefficient
a	receptor physical radius
R	receptor effective radius
$\forall(x, y)$	for all points (x, y) on the membrane surface
$\in \mathcal{R}$	belonging to domain $\mathcal{R}$
Δx	grid spacing along x-axis
Δy	grid spacing along y-axis
Δt	simulation time step
E	magnitude of applied electric field
f	frequency of the sinusoidal field
$C^t_{x,y}$	receptor density within a grid area around (x, y) at time t
C^0	initial uniform density of receptors
$C_{m_{x,y}}$	density of mobile receptors
$C_{im_{x,y}}$	density of immobile receptors
I_{im}	immobile fraction
C_{max}	maximum receptor density
ΔV_m	transmembrane potential
ψ_{ind}	induced membrane potential
ψ_0	resting extracellular surface potential
C_b	ionic concentration in bulk aqueous phase
ϵ	dielectric constant of the aqueous medium
F_i	initial fluorescence
F_∞	equilibrium fluorescence
$\lfloor Z \rfloor$	greatest integral value less than or equal to Z

INTRODUCTION

Electrical phenomena govern many biological processes from molecular binding interactions to intercellular communication. Endogenous or exogenous perturbations of physiological fields by small extracellular electric fields have been observed to affect cellular processes, and several different mechanisms for these effects have been proposed (Weaver and Astumian, 1990). Some investigators have observed that sinusoidal electric fields alter fundamental cellular functions (Goodman et al., 1983; McLeod et al., 1987); such studies have led to concern about potential biological hazards from exposure to environmental sinusoidal fields. Most of the proposed coupling mechanisms are the subject of substantial debate. Motivated in part by this debate, we examined the effect of sinusoidal electric fields on a well-established mechanism of field-cell coupling that involves redistribution of charged cell surface receptors.

Many receptor types are mobile within the plane of the plasma membrane (Schlessinger et al., 1978; Wolf et al., 1980; Poo, 1981; Edidin and Wei, 1982; McCloskey et al., 1984; Menon et al., 1986). Surface receptor redistribution is involved in cellular processing of many types of ligands. Events that modulate receptor transport and distribution may then affect cell behavior. Because plasma membrane constituents also include electrically charged lipids and glycoproteins, an electric field can drive receptor migration by both electroosmosis and electrophoresis (McLaughlin and Poo, 1981). Jaffe and Nuccitelli (1977) reported that direct current (dc) fields as small as 10 V/cm, applied parallel to the cell surface, cause substantial redistribution and crowding of charged macromolecules in the plane of the plasma membrane.

Transport kinetics

Because of the relatively small electromigration mobility of most receptors (Poo, 1981), the kinetics of field-in-

Address correspondence to Dr. Raphael C. Lee, Department of Surgery, MC 6035, The University of Chicago Medical Center, 5841 South Maryland Avenue, Chicago, IL 60637, USA.

0006-3495/93/01/044/14 $2.00

duced molecular crowding is very slow compared with the other known mechanism of protein mediated electrochemical coupling, i.e., ion channel gating. For example, it has been reported that application of a 4-V/cm dc electric field causes redistribution (capping) of cell surface concanavalin A (con A) receptors to one of the poles of living *Xenopus* muscle cells (Poo and Robinson, 1977) in a 20-min interval; Poo (1981) found that 10 min were required for a 10-V/cm dc field to accumulate con A receptors at the cathode pole of *Xenopus* muscle cells. Guigni et al. (1987) observed that a dc field of 15 V/cm induces redistribution of epidermal growth factor receptors such that the concentration of receptors at the cathode pole is tripled over a 30-min period.

Conceptually, application of a sinusoidal electric field is likely to lead to a sustained cellular response mediated by receptor electromigration only if there is a net time-average displacement of receptors. In effect, rectification of receptor transport must occur. For flat cells that can reasonably be viewed as having a two-dimensional geometry, three potential mechanisms of rectification could lead to a time-average receptor displacement. These mechanisms include the effects of protein crowding, anisotropic membrane properties, and asymmetry in cell surface geometry relative to the electromigration path. Another mechanism relevant to a spherical cell in a uniform field could involve field nonuniformity over the cell surface (Zimmermann, 1982).

Receptor crowding

Receptor crowding affects the redistribution of receptors in an applied field. In theory, either large fractions of immobile receptors or high concentrations of mobile particles cause slowing of protein diffusion by as much as several orders of magnitude (Saxton, 1982, 1987; Eisinger and Halperin, 1986). Saxton (1987) used Monte Carlo simulations to show that this strong dependence of receptor diffusivity on concentration is principally related to finite molecular size and excluded volume effects. Similarly, Ryan et al. (1988) successfully accounted for receptor crowding effects by using a solid volume exclusion principle describable by the Fermi-Dirac statistical model. In reconstituted artificial membranes, high protein-to-lipid ratios have been shown to slow lateral diffusion of both bacteriorhodopsin and gramicidin C (Tank et al., 1982; Peters and Cherry, 1982; Vaz et al., 1984). Field-induced movements of mobile particles are also slowed by immobile molecules with cytoplasmic attachments to cytoskeletal structures (Peters and Cherry, 1982; Saxton, 1987), by large molecular aggregates, or by immiscible domains of membrane lipids. For example, Fc receptors on rat basophilic leukemia cells (Ryan et al., 1988) and con A receptors on *Xenopus* myotomal cells (Poo and Robinson, 1977) have mobile fractions of 0.7 and 0.5, respectively.

Alteration in membrane surface charge

Gross et al. (1983) and Gross (1988) have pointed out that electromigration related redistribution of charged membrane receptors alters the transmembrane potential (ΔV_m) due to accompanying shifts in membrane surface charge density. The effect of surface charge redistribution on ΔV_m often opposes the direct induced membrane potential (ψ_{ind}) imposed by the field. As noted by Gross (1988), a unidirectional extracellular field is likely to cause a biphasic change in ΔV_m. The initial response results from the directly imposed transmembrane potential and the later response to electrophoretic redistribution of charged surface receptors.

Evidence for anisotropy of receptor mobility

Anisotropic receptor mobility on flat (~two-dimensional) cells has been demonstrated in at least two reports. Smith et al. (1979) showed that succinyl con A receptors diffuse anisotropically on murine fibroblasts with the more rapid diffusion in a direction parallel to the underlying actin stress fibers. Stolpen et al. (1988), using the "line FPR" technique, found that human dermal fibroblasts exhibit anisotropic diffusion of class I major histocompatibility complex (MHC) proteins, with transport faster along the direction of cytoplasmic stress fibers and slower perpendicular to the stress fibers.

Net cell surface receptor transport under an applied electric field is governed by the sum of electromigration and diffusive fluxes. Because mutual diffusion depends on the surface width available for diffusion, diffusive transport is strongly dependent on cell geometry. If there is no line of symmetry normal to the direction of receptor electromigration, then the dependence of mutual diffusion on cell geometry could lead to an effective uniaxial anisotropy in resistance to receptor movement. Under such conditions, the time-average distribution of receptors would be altered such that the center of mass of surface receptors shifts from its location before the application of a field. The magnitude of this effect under an applied sinusoidal electric field depends only on cell shape and orientation of the cell's major axis with respect to the field.

Cell shape–dependent rectification

This theoretical and experimental evidence for anisotropy of receptor mobility led us to postulate that a sinusoidal electric field could effect a net time-average displacement of receptors on the surface of isotropic cell membranes, thereby shifting the center of mass of such receptors and effectively rectifying receptor transport. The subsequent redistribution of charged surface components also could be expected to lead to a change in transmembrane potential. ΔV_m would be greatest at locations on the cell surface that experience a large change in receptor concentration due to the applied sinusoidal field.

One objective of the present study was to gain a quantitative understanding of steady-state redistribution of charged cell surface receptors under an applied field. This objective was achieved by solving the electromigration-diffusion equation. Analytical solutions for spherical and cylindrical cells have been reported (Young et al., 1984). In the case of a cell of irregular geometry, however, the existence of an analytical solution is unlikely. Instead, the partial differential equation describing receptor transport with a set of initial and boundary conditions can be solved using the finite difference technique. This method of analysis is less intensive in computation relative to other methods; it allows great flexibility in incorporating into the model various biophysical features that characterize protein movement and it is robust for cells of arbitrary shape. The model was validated by comparison with experimental values at equilibrium (Ryan et al., 1988) and under dynamic conditions.

MATERIALS AND METHODS

Receptor transport on the cell surface in an applied electric field was modeled based on the finite difference method. The effect of transport parameters on receptor movement was studied in a series of computer simulations. Anisotropy in receptor transport on an asymmetrically shaped cell was verified experimentally. The materials and methods involved in simulation and experiment are discussed.

Simulation methods

Formulation of the model

In an electric field E, a charged molecule migrates with speed $U = \mu E$, where μ is the effective electromigration mobility (Young et al., 1984). This mobility reflects both electrophoretic and electroosmotic effects (McLaughlin and Poo, 1981). Redistribution of surface receptors is then considered as a balance between two migratory fluxes in the plane of the cell membrane: a unidirectional electromigration resulting from the net force produced by field-related processes and a diffusional flux in the opposite direction that tends to randomize the electromigration-induced, nonuniform distribution. These fluxes are characterized by mobility parameters that are assumed to be isotropic throughout the cell surface: the effective electromigration mobility μ and the diffusion coefficient D (Young et al., 1984).

Following the Saffman–Delbrück model (Saffman and Delbrück, 1975), protein molecules of 5 nm diameter (e.g., corresponding to bacteriorhodopsin [Peters and Cherry, 1982]) were assumed to be uniformly distributed over the membrane surface in the absence of an applied field. Because lateral movement of molecules is confined to the cell surface, receptors were modeled as identical, hard disks that were assumed to occupy ~20% of all accessible sites on the cell (Golan et al., 1984) with an immobile fraction of 30% (Stolpen et al., 1988). Class I MHC protein movement in fibroblast plasma membranes, experimentally found to be described by a diffusion constant of 2.3×10^{-9} cm^2/s and an effective electromigration mobility of 1.2×10^{-6} cm^2/V-s (Basch, 1988; Stolpen et al., 1988), was used to model D and μ.

The distribution of charged membrane components in an applied electric field can be described by the continuity equation (Poo, 1981):

$$\partial C/\partial t = D\nabla^2 C - \mu(\nabla C)\cdot \mathbf{E}, \qquad (1)$$

where $C \equiv C(x, y, t)$ is the surface density of membrane components in a finite area surrounding a point (x, y) on the cell surface at time t, $\mathbf{E}$ is the electric field vector over the cell surface at (x, y). For a sinusoidal electric field $E \sin(\omega t)$, where $\omega = 2\pi f$ and f is the frequency of the sinusoidal field, the distribution of surface components is described by

$$\partial C/\partial t = D\nabla^2 C - \mu(\nabla C)\cdot E \sin(\omega t). \qquad (2)$$

The time-averaged profiles of receptor concentration shown in this article are plots of average concentration values over one complete cycle of sinewave after sinusoidal steady state has been reached.

The finite difference technique was used to solve Eq. 2. The finite difference representation of the electromigration-diffusion equation can be written as (Hildebrand, 1968):

$$C^{t+\Delta t}_{x,y} = C^t_{x,y} + \Delta t\cdot\frac{D}{(\Delta x)^2}(C^t_{x+\Delta x,y} - 2C^t_{x,y} + C^t_{x-\Delta x,y}) + \Delta t\cdot\frac{D}{(\Delta y)^2}(C^t_{x,y+\Delta y} - 2C^t_{x,y} + C^t_{x,y-\Delta y}) - \Delta t\cdot\frac{\mu E_x}{\Delta x}(C^t_{x,y} - C^t_{x-\Delta x,y}), \qquad (3)$$

where $C^t_{x,y}$ is the receptor concentration at time t in a surface membrane compartment of area $\Delta x\cdot\Delta y$ around the point (x, y). Eq. 3 was subjected to the boundary condition $\hat{\mathbf{u}}\cdot\nabla C = 0$, where $\hat{\mathbf{u}}$ is a unit vector perpendicular to the membrane surface and pointing outward of the boundary (i.e., the receptors are constrained to the cell surface) and to the initial condition $C^0_{x,y} = C^0, \forall(x, y) \in$ cell (i.e., for all points $[x, y]$ within the cell). In solving the finite difference equation, an outline of the cell under analysis was traced from a photomicrograph of the cell onto a uniform two-dimensional grid. The spacing of the uniform grid was 0.2 μm. The cell length and width were 40 and 5–20 μm, respectively. The spacing between adjacent grid points was chosen so that there were no discontinuities near the cell boundary. The electromigration-diffusion equation was solved for the whole cell by iteratively computing the flux of molecules across the grid areas in each consecutive finite time interval until equilibrium was reached. Equilibrium was assumed when the time-average concentration showed <5% variation compared with the previous cycle. $C^t_{x,y}$, the concentration of receptors within the grid area around the point (x, y), was assumed to contain both mobile and immobile receptors, i.e., $C^t_{x,y} = C^t_{\mathrm{m}_{x,y}} + C^t_{\mathrm{im}_{x,y}}$. The number of immobile receptors was given by $C^t_{\mathrm{im}_{x,y}} = I_{\mathrm{im}}\cdot C^0$, $\forall(x, y) \in$ cell, where C^0 was the initial uniform concentration and I_{im} was the immobile fraction.

Implementation of steric exclusion and space saturation constraints

Ryan et al. (1988) showed that, at high protein concentrations, protein–protein interactions in the cell membrane lead to saturation of the diffusible area on the cell. To account for this effect, steric volume exclusion was invoked in our finite difference model. Movement of receptors was restricted by imposing the condition that a receptor on the surface of a cell membrane could not approach another receptor closer than its own effective radius that is determined by a combination of steric, binding, and electrostatic interactions (Lauffer, 1989). Fig. 1 shows how receptor excluded volume was accounted for in the model. Receptors (of physical radius a) were treated as hard cylinders with effective radius R, where $R > a$.

The steric exclusion rule was invoked after every iteration to limit the number of molecules in each grid area. The maximum receptor concentration that could be accommodated within a grid area was given by

$$C_{\max} = \lfloor 2\Delta x\Delta y/3\pi R^2 \rfloor. \qquad (4)$$

"Saturation" of the grid area at (x, y) occurred when the number of receptors driven toward the grid from adjacent elemental areas exceeded the number that could be accommodated within the grid area. Specifically, receptors could enter and leave grid areas due to diffusion and/or field-induced migration. The number of receptors that *entered*

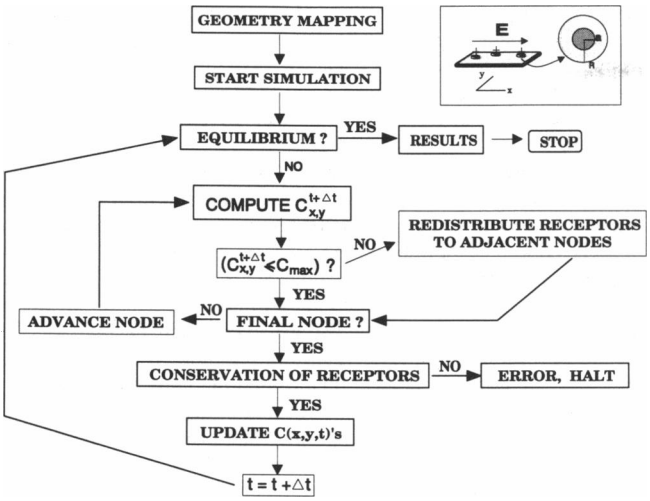

FIGURE 1 Flowchart of simulation algorithm. The excluded volume effect is incorporated into the model by using an effective radius R for the receptor.

the grid area centered at (x, y) from an adjacent grid element $(x + k, y + l)$ during an interval Δt was ${}_iC_{x+k,y+l}$. Similarly, the number of receptors that *left* the grid area around (x, y) to an adjacent grid area around $(x + k, y + l)$ was ${}_oC_{x+k,y+l}$. Then, the grid area around (x, y) was saturated (accounting for steric exclusion) if

$$C_{T_{x,y}} + C^t_{m_{x,y}} + C^t_{im_{x,y}} \geq C_{max}, \tag{5}$$

where

$$C_{T_{x,y}} = \sum_{k,l} ({}_iC_{x+k,y+l} - {}_oC_{x+k,y+l}), \quad \begin{cases} k = -\Delta x, 0, \Delta x \\ l = -\Delta y, 0, \Delta y \\ k = l \neq 0 \end{cases} . \tag{6}$$

In the event of saturation, the number of receptors entering the elemental area around (x, y) from each of its neighboring elements was proportionally limited to

$${}_iC^{limit}_{x+k,y+l} = {}_iC_{x+k,y+l} \cdot \frac{C_{max} - (C_{T_{x,y}} + C^t_{m_{x,y}} + C^t_{im_{x,y}})}{\sum_{k,l} {}_iC_{x+k,y+l}}, \quad \begin{cases} k = -\Delta x, 0, \Delta x \\ l = -\Delta y, 0, \Delta y \\ k = l \neq 0 \end{cases} . \tag{7}$$

Receptor concentration within each grid area was updated after every iteration, simultaneously checking for conformance to the space saturation constraint and conservation of cell surface receptors. If the receptor conservation condition was violated, then the simulation was halted.

Calculation of transmembrane potential

Redistribution of charged macromolecules on the surface of a cell leads to alterations in transmembrane potential because of shifts in the membrane surface potential (ψ) (Gross, 1988). The transmembrane potential (ΔV_m) was calculated as:

$$\Delta V_m(x, y) = -\Delta\psi(x, y) + \psi_0 + \psi_{ind}(x, y), \tag{8}$$

where ψ_0 is the resting potential, $\Delta\psi(x, y)$ is the change in surface potential at point (x, y) due to redistribution of receptors, and $\psi_{ind}(x, y)$ is the peak membrane potential induced directly by the peak applied field E in the positive direction. Because the time averaged ψ_{ind} is zero over one cycle of the sinusoidal field, peak ψ_{ind} is used to calculate the maximum ΔV_m experienced by the cell membrane. Net changes in V_m depend on the signs and relative magnitudes of the inner and outer surface potentials, the fraction of mobile charged components on the two membrane faces, and the electrical properties of the cell and its surroundings (Gross, 1988). The variation of intracellular surface potential with an applied field was assumed to be negligibly small. We used the expression of transmembrane potential change in terms of steady-state concentration of redistributed macromolecules developed by Gross (1988):

$$\Delta V_m(x, y) = -\left(2\frac{RT}{F}\right) \cdot \sinh^{-1}\left\{\frac{\sigma_0}{A}\left(\frac{C_\infty(x, y)}{C_0}\right)\right\} + \psi_0 + E \cdot d, \tag{9}$$

where d is the distance from the point (x, y) to the origin (assumed to be located at the center of the cell), $C_\infty(x, y)$ is the steady-state concentration (time-averaged over 1 cycle in the case of a sinusoidal field), σ_0 is the initial uniform extracellular surface charge, R is the gas constant, and T is the absolute temperature. A was calculated as

$$A = (8C_b\epsilon RT)^{1/2}, \tag{10}$$

where C_b is the ionic concentration in the bulk aqueous phase and ϵ is the dielectric constant of the aqueous medium near the membrane surface.

The protein transport simulation was implemented on a VAXstation 3540 computer (Digital Equipment Corp., Marlboro, MA) under the VMS 5.3 operating system environment. The simulation program was written in C. A flowchart of the simulation program is shown in Fig. 1. Both symmetrical and asymmetrical cell geometries were used in the series of simulations designed to study receptor transport under an applied sinusoidal field. Symmetry in surface geometry was defined with respect to an axis normal to the direction of electromigration.

The time increment corresponding to each iteration, Δt, was chosen such that the sampling frequency was an order of magnitude greater than the Nyquist frequency to avoid temporal undersampling of the input sinusoidal field. In addition, to avoid oscillations and to ensure convergence of the solution, it was necessary to restrict the time interval to satisfy the stability criterion (Press et al., 1986). Thus, Δt had to satisfy the two constraints:

$$\Delta t \cdot f \geq 0.01,$$

and

$$\Delta t \leq \min\{(\Delta x)^2/2D, \quad (\Delta y)^2/2D\}, \tag{11}$$

where f is the frequency of the applied sinusoidal field. This condition implied that the time interval was required to be smaller than the mean time for Brownian diffusion to an adjacent grid element.

Experimental methods

Postfield receptor back-diffusion in fibroblast cell membranes

Back-diffusion rates for class I MHC proteins in cell membranes of human dermal fibroblasts were measured experimentally by monitoring the diffusive relaxation kinetics after an applied dc field was turned off. In this method, cell surface fluorescence intensity was monitored in a 1-μm radius spot located at a selected point near the leading edge on the major axis of the fibroblast. Application of an electric field caused the initially uniform concentration of charged macromolecules to become nonuniform by accumulation at one pole of the cell. Removal of

the field allowed diffusion of proteins to restore a uniform surface distribution. When the polarity of the field was reversed, receptors accumulated at the opposite pole of the cell. Characteristic post-field back-diffusion times were determined after application and removal of both "+" and "−" polarity fields.

Primary human dermal fibroblast cultures were obtained through collagenase digestion of neonatal foreskin tissue. The digested tissue was then washed twice in sterile phosphate-buffered saline (PBS) solution without calcium and magnesium. To remove endothelial cells, the tissue was placed in a 50-ml centrifuge tube with 20 ml of hydrated 10× trypsin solution and 0.025% EDTA and incubated for 15 min. The tissue was then cut into small pieces and placed in sterile Dulbecco's modified Eagle's medium (DMEM) with 0.4% collagenase, penicillin (10,000 U/ml), and streptomycin (10,000 μg/ml). It was then incubated at 37°C and agitated for 4 h. After tissue digestion, the cells were suspended in DMEM, washed twice by centrifugation to remove all collagenase, and then seeded in flasks at a density of 10^8 cells/25 cm^2.

Cells were grown to 80% confluence, passed twice, and stored at a cell density of $\sim 10^6$ cells/ml in preservation medium consisting of 5% calf serum, 45% DMEM, and 50% dimethylsulfoxide at −100°C. One milliliter of cell suspension was thawed, and cells were plated in a T75 culture dish and allowed to grow to 80% confluence. Approximately 72 h before each experiment, $\sim 2.5 \times 10^5$ cells were passed into 15-mm petri dishes containing a sterile 24 × 35-mm microscope coverslip. Six milliliters of DMEM with 10% calf serum and 200 U/ml recombinant human immune interferon (IFN-γ) [HG-IFN; Genzyme, Cambridge, MA] were added to each dish. IFN-γ was used to induce increased expression of class I MHC proteins (Stolpen et al., 1988). IFN-γ was stored frozen at −100°C in aliquots containing 10,000 U in 10 μl. The coverslips were placed in a sterile chamber and incubated with 5 ml DMEM with 10 mM *N*-2-hydroxyethylpiperazine-*N'*-2-ethane sulfonic acid, 10% calf serum, and 200 U/ml IFN-γ. Cultured fibroblasts were ~50 μm long and were typically quasi-two-dimensional (flat) in shape and characterized by unequal principal axes.

Cell surface class I MHC proteins were labeled with W6/32, an immunoglobulin G_{2a} monoclonal antibody, directed against a monomorphic determinant of human histocompatibility leukocyte antigens-A, B, C (Barnstable et al., 1978), conjugated to fluorescein-isothiocyanate (FITC) (Stolpen et al., 1988). Cells on a coverslip were gently washed two or three times in PBS with calcium and magnesium at room temperature. The coverslip was then placed on ice in a staining chamber containing 1.4 ml DMEM and 100 μl fluoresceinated antibody solution (final antibody concentration 50–100 μg/ml). A 26.0 × 36.5-mm well in a polysulfone block served as the staining chamber. After incubation with antibody for 1 h, the coverslip was washed twice in PBS without calcium and magnesium to remove most of the membrane-bound calcium and the unbound antibody. The coverslip was then mounted cell side down on an exposure chamber that was filled with PBS without calcium and magnesium.

The chamber used to expose the cells to the field was made from polysulfone, an autoclavable electrical insulator. The chamber was designed to limit heating and prevent electrode reaction products from reaching the cells. The chamber was similar to that illustrated by Gross et al. (1986) and is described by Basch (1988). To prevent Joule heating by extracellular currents, a small amount of silicon grease was used to mount the coverslip 250 μm above an optically polished sapphire window (Adolf Miller, Providence, RI) that served to separate cells and media from a second chamber containing circulating cooled nitrogen. Sandwiched between the thin coverslip and the sapphire window was a foil type-T copper-constantan thermocouple (20102-1 Rdf Corp., Hudson, NH). Sapphire was chosen because of its high thermal conductivity and optical transparence. The foil type thermocouple was used because it is only 5 μm thick and operates over a temperature range of −150–400°C. To prevent cell contact with undesirable electrochemical byproducts at the electrodes, the field exposure area of the chamber was separated by media bridges. Assuming that heat was not conducted between air and media, the media temperature rise per unit time was computed to be 0.19°C/s for a field strength of 10 V/cm. Control experiments showed an initial rise of temperature of ~0.1°C/s and a maximum change of 4–5°C above room temperature. The stream of nitrogen gas under the sapphire plate, cooled through a heat exchanger in ice water, was used to counter this temperature rise. A hand-controlled valve regulated the flow of nitrogen to keep the media at room temperature.

The laser microscope apparatus has been described in detail (Golan et al., 1986). A 63× microscope objective and 350-mm focal length lens were used to form a Gaussian beam of radius ~1.3 μm at the sample plane. The monitoring beam was used to measure fluorescence intensity at a location near the leading edge of the cell. Measurements were performed near the cell boundary to maximize changes induced by the applied field. FITC-W6/32–labeled cells were exposed to a 10-V/cm field until a significant change in receptor surface density was observed. Removal of the field then caused the fluorescence intensity to return to its initial value, and the kinetics of diffusion were determined from the intensity time profile. The procedure was repeated with an electric field of the same magnitude but with opposite polarity. Data were fitted to an exponential function that describes the fluorescence profile at any point on the cell:

$$F(t) = (F_i - F_\infty)e^{-t/\tau} + F_\infty, \tag{12}$$

where F_i is the initial fluorescence, F_∞ is the final (uniform) fluorescence, and τ is the first order rate constant for back-diffusion. Thus, the time constants of back-diffusion after removal of positive and negative electric fields were obtained by fitting the back-diffusion data to an exponential function. The time constants of protein transport after the application of negative and positive electric fields are denoted by τ_+ and τ_-, respectively. The exact length of each cell was difficult to determine because cells were irregularly shaped. Since an error in estimation of cell length affects the value of the diffusion coefficient as the square of the error, the ratio of the two diffusion coefficients was considered to represent the best experimental measure of uniaxial anisotropy. The extent of uniaxial anisotropy was quantified by the extent to which the ratio

$$D_+/D_- = \tau_-/\tau_+, \tag{13}$$

deviated from unity. The mean and standard deviation of diffusion time constants were determined from a set of eight experiments.

MODEL CALIBRATION

The effects of cell shape, electric field, and protein mobility on the transport of cell surface receptors in response to an applied electric field were studied using the finite difference model. The validity of the model was established by comparing the simulation results with previously published theoretical and experimental values. The model was then tested against experimental results of class I MHC protein transport in plasma membranes of human dermal fibroblasts.

The analytical solution of the electromigration-diffusion equation for a perfectly rectangular cell geometry at equilibrium is given by:

$$C(x) = \frac{\mu E C^0 l}{D(\exp^{[(\mu E/D)l]} - 1)} \exp^{[(\mu E/D)x]}, \tag{14}$$

where l is the cell length and x is the distance from the trailing edge of the cell. The finite difference model predictions were compared with the results obtained by using this analytical solution, in both cases assuming that

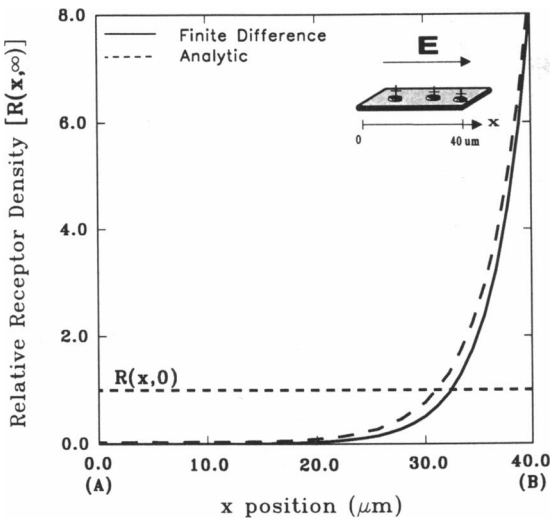

FIGURE 2 Comparison between prediction of finite difference model and that of the analytical solution (Eq. 14) at equilibrium for a rectangular surface. Receptors were assumed to have an effective electromigration mobility of 1.2×10^{-6} cm^2/V-s and a lateral diffusion coefficient of 2.3×10^{-9} cm^2/s. Applied dc field strength was 10 V/cm. Root mean square (rms) difference between the profiles is ~7%.

all receptors were infinitely small and that all receptors were mobile. $C(x)$ obtained by the analytical and finite difference methods corresponded closely (Fig. 2). The root mean square deviation between the two profiles was 7.4%.

A second calibration was implemented by comparing predictions of the finite difference model with theory and experimental values published by Ryan et al. (1988). The equilibrium distribution of infinitely small receptors on a cell in a potential gradient can be described by the Boltzmann probability distribution. A large discrepancy was observed by Ryan et al. (1988) between predictions of the Boltzmann model and experimental results on spherical cells, however. The predictions of the finite difference model for the relative receptor surface concentration profile as a function of angle θ with respect to the direction of the dc applied field is shown for different field strengths in Fig. 3 *a*. Assuming infinitesimal or finite receptor size, the results closely correspond to those predicted by the Boltzmann or Fermi–Dirac distribution, respectively (Ryan et al., 1988). These results, obtained using the values for immobile fraction and fractional occupancy measured by Ryan et al. (1988), validate the model against both experimental data and an equilibrium statistical model. The finite receptor size model shows a density ceiling near the leading edge of the cell (i.e., at $\theta = 180°$), due to crowding of receptors and consequent reduction in the number of accessible sites available for a given protein molecule (Fig. 3 *b*). The uneven change in concentration profile near $\theta = 90°$ and $\theta = 270°$ at low field strengths is due to the discretization error resulting from the planar projection of the cell. Both the finite difference simulation and the Fermi–Dirac model predict that saturation of accessible sites limits the maximum receptor density at the cathodal pole to a value less than that attained assuming infinitesimal receptor size. Fig. 3 *c* is a surface plot that shows this effect of saturation on the steady-state receptor distribution.

RESULTS

Simulation of dynamic responses

As anticipated, the model predicted that receptor mutual diffusion kinetics are dependent on surface geometry. Because the electromigration mobility is independent of cell geometry, we initially explored the effects of cell shape on back-diffusion kinetics. The effects of shape on mutual back-diffusion are shown in Fig. 4. The plots show the evolution of receptor surface density at two points on a rhomboid-shaped surface 40 μm in length. One point (A) was located at the narrow apex and the other (B) at the broad apex as shown. In this simulation, a 10-V/cm field was applied to cause receptor crowding at one end of the wedge-shaped surface. The field was applied until the receptor density distribution reached equilibrium. The field was then turned off to let the receptors diffuse back to the initial uniform distribution. The characteristic back-diffusion time for this asymmetrical geometry was clearly dependent on the direction of back-diffusion. This uniaxial anisotropy in protein transport (manifested as significant differences in characteristic times for diffusion and in magnitudes of peak displacement at the two points) was observed only for surface geometries that were asymmetric along the axis of receptor electromigration. For the surface geometry displayed in Fig. 4, the back-diffusion time constants differed by ~20% between the two points.

Rectification of receptor electromigration in a sinusoidal field

As illustrated by a comparison between the history of receptor surface densities assuming two different surface geometries (Fig. 5 *a*), the instantaneous receptor density at any point on the surface depended not only on the magnitude and sign of the applied sinusoidal field but also on the receptor density evolution. Both surface shapes shown were subjected to a 0.1-Hz sinusoidal electric field of 10 V/cm, assuming a receptor immobile fraction of 30%, diffusion coefficient of 2.3×10^{-9} cm^2/s and electromigration mobility of 1.2×10^{-6} cm^2/V-s. The receptor density evolutions shown in Fig. 5 *a* correspond to instantaneous densities at two points (*A* and *B*) at the apices of a symmetrical (left) and an asymmetrical (right) rhomboid surface, respectively. The initial transient change in receptor density was up to fourfold greater than the steady-state peak density. The time-

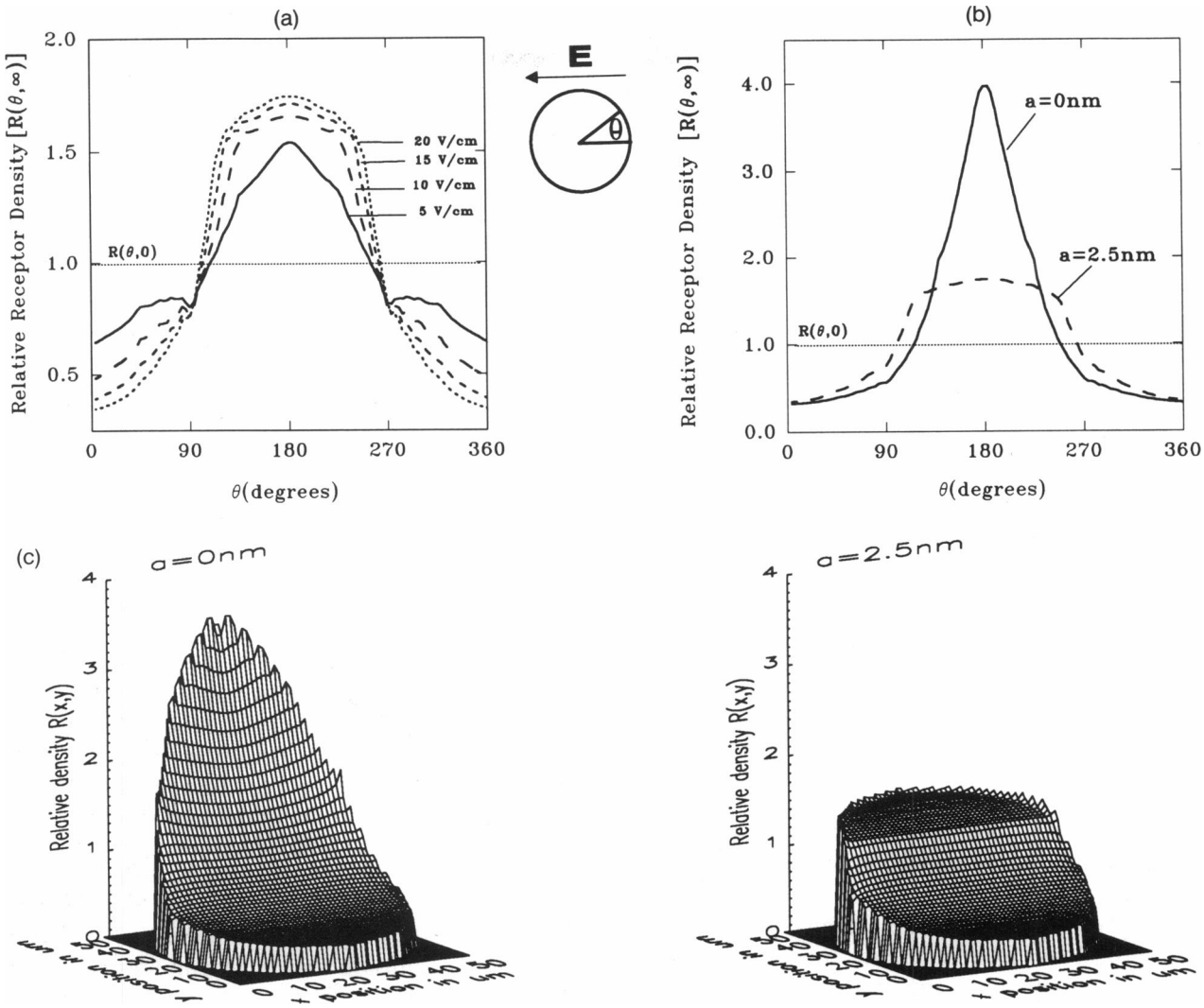

FIGURE 3 (*a*) Finite difference solution for the effect of dc field strength on the equilibrium distribution of receptors on a 50-μm spherical cell. Receptors were assumed to have an effective electromigration mobility of 1.2×10^{-6} cm^2/V-s and a lateral diffusion coefficient of 2.3×10^{-9} cm^2/s. At low field strengths, the distribution followed the Boltzmann distribution. The concentration profile deviated from the ideal distribution at higher field strengths due to *saturation* of the diffusible area for receptors. These results agree well with the theoretical and experimental results of Ryan et al. (1988). (*b*) Effect of finite receptor radius (*a*) on the equilibrium normalized concentration of cell surface receptors. Applied dc field strength was 20 V/cm. The effect of *saturation* was to reduce the peak shift in concentration from that obtained by using the ideal Boltzmann distribution. The distribution of receptors instead followed a Fermi–Dirac distribution when the finite size of receptors was taken into account. (*c*) Surface plots comparing the Boltzmann solution (*A*) to predictions of the finite difference model (*B*). This comparison underscores the importance of finite receptor size on receptor transport.

average densities (over 1 cycle of the sinusoidal field at steady state) converged to nearly the same value at the two ends of the symmetrical surface geometry (note that the two instantaneous values were 180° out of phase), whereas those at the two ends of the asymmetrical surface geometry converged to values that were different by ~30%.

When the surface geometry was symmetrical, no shift in receptor center of mass occurred. In the case of the asymmetrical geometry, there was a shift in receptor center of mass; in effect, this shift represented rectification of the response. The difference between receptor surface densities at opposite ends of an asymmetrical geometry was a function of the degree of asymmetry. Fig. 5 *b* is a surface plot that shows this effect.

The dependence of receptor redistribution on the magnitude of receptor mobility is illustrated in a plot of the steady-state time average receptor density along the axis of receptor electromigration on an asymmetrical rhomboid surface (Fig. 6 *a*). The extent of receptor accumulation at point *A* (the narrow apex) was found to be greater for receptors with higher mobility. The smallest mobility value used in these calculations was that experimentally measured for class I MHC proteins on neonatal human dermal fibroblasts (Basch, 1988). A sharp increase in the level of receptor redistribution was

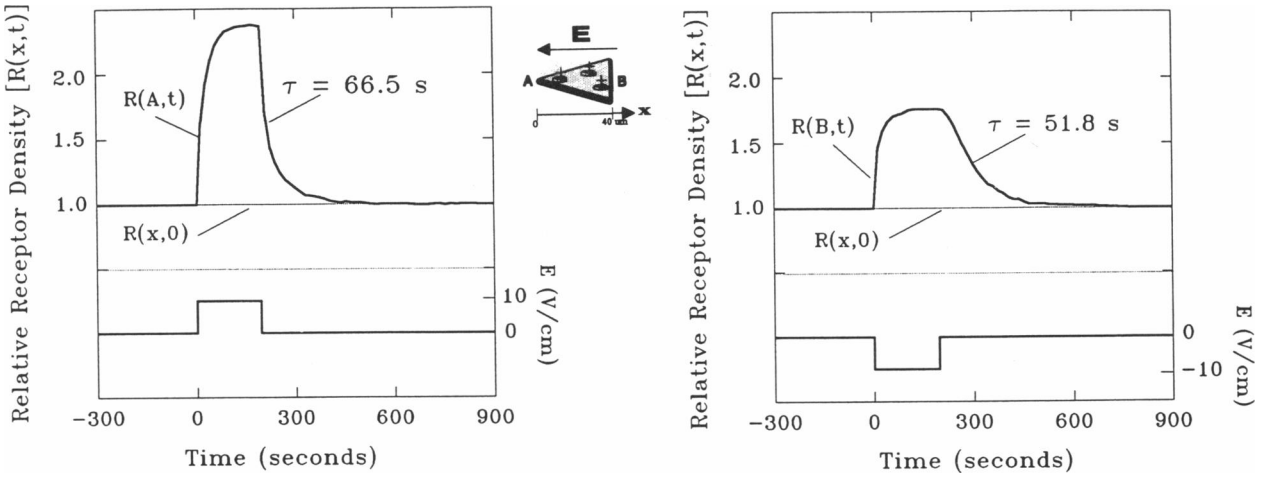

FIGURE 4 Effect of cell shape asymmetry on back-diffusion time constants for receptors at equilibrium after application of a dc field. Receptor density was calculated at two points (*A* and *B*) on a rhomboid-shaped surface before, during and after application of a 10-V/cm pulse. The time constants for receptor back-diffusion after removal of the field are shown for both polarities. Receptors were assumed to have an effective electromigration mobility of 1.2×10^{-6} cm^2/V-s and a lateral diffusion coefficient of 2.3×10^{-9} cm^2/s.

observed in the millihertz frequency range for D/μ ratios < 1 mV.

Frequency response

The dependence of receptor transport on field frequency is illustrated in Fig. 6 *b*. A decrease in the magnitude of time-average net receptor displacement was observed at higher frequencies. Receptor accumulation in an applied sinusoidal field could be conceptually categorized as a low-pass filter. For receptors with an electromigration mobility of 1.2×10^{-6} cm^2/V-s, significant accumulation at the apices was noted at a frequency of 10 mHz. Rectification of receptor distribution required sub-millihertz frequencies, however. As anticipated, these cutoff values were sensitive to surface geometry and to receptor mobility parameters. Shortening the surface length in the field direction caused the frequency roll-off to shift toward higher frequency. Increasing receptor diffusibility to values characteristic of membrane lipids (10^{-8} cm^2/s) caused rectification of receptor transport to occur at frequencies as high as 0.1 Hz. The effects of cell shape on receptor transport were most prominent at very low frequencies. At 0.1-mHz frequency and 10-V/cm field strength, an asymmetrical surface geometry showed a difference of >2.5 in the steady-state time-average receptor density at opposite poles of the geometry.

Transmembrane potential distribution

The shift in transmembrane potential (Eq. 9) along the major axis of an asymmetrical geometry in response to an applied sinusoidal field of 0.1-mHz frequency is shown in Fig. 7. Above this cutoff frequency, changes in transmembrane potential resulted solely from the induced field, since applied fields of such frequencies caused minimal receptor redistribution. Below the cutoff frequency, however, the effects of altered surface charge were found to be substantial. At very low frequencies, alterations in transmembrane potential induced indirectly via surface charge redistribution could be greater than the directly induced transmembrane potential by as much as an order of magnitude (Fig. 7). The magnitude of the surface charge component of transmembrane potential was dependent on the magnitude of receptor mobility, the amplitude and frequency of the applied field, and the shape of the cell. For example, the magnitude of the surface charge effect was reduced by the presence of immobile surface components that served to hinder the movement of mobile receptors.

Comparison between experiment and theory

The surface density of FITC-W6/32–labeled class I MHC proteins was monitored at a selected point near the leading edge of individual human dermal fibroblasts in culture (Fig. 8). The electric field pulse sequence shown in Fig. 8 was used to measure the characteristic back-diffusion times in opposite directions of electromigration. To ensure that the result was not a consequence of the initial direction of the field, the initial field polarity was reversed in half the experiments; no dependence on initial polarity was observed. Maximum changes in fluorescence intensity were observed when the monitoring spot was close to the edge of the cell. Uniaxial anisotropy of receptor transport was quantified experimentally by measuring the ratio of back-diffusion time constants after application of + and − dc electric fields. The table of data in Fig. 8 (*right*) shows the measured values of back-diffusion times for eight independent experiments, their ratios, and the least-squared error of the fit to the

exponential. The average ratio of τ_-/τ_+ was 1.35 ± 0.46. This ratio corresponded to $P < 0.025$ in a two-tailed Student's t test, indicating a >99.75% probability that τ_- and τ_+ were actually different.

The asymmetrical fibroblast geometry shown in the inset of Fig. 8 was used in the finite difference simulation to compare the model directly with experimental results. The cell for which the simulation was performed was 40 μm in length and had receptors of electromigration mobility 1.2×10^{-6} cm^2/V-s and diffusion coefficient 2.3×10^{-9} cm^2/s (Basch, 1988). The predicted relative receptor density at the leading edge of the cell with the field turned off was fit to an exponential function to obtain predicted time constants for back-diffusion. The ratio τ_-/τ_+ for this asymmetrical geometry was determined to be 1.625, in good agreement with the experimental results.

DISCUSSION

The finite difference model used in this study provided a highly practical means for studying lateral transport of membrane-bound proteins on cells of irregular shape. This method can be a useful tool when closed-form analytical solutions are nonexistent and when Monte Carlo simulations (e.g., Pink et al., 1986; Saxton, 1987) and fractal methods are computationally intensive. Various characteristics that modulate protein movement in an applied electric field can be incorporated into the model. Such factors include the presence of immobile molecules; finite receptor size; excluded membrane area; cell shape; and the magnitude, orientation, and frequency of an applied sinusoidal electric field. The electromigration mobility value used in the simulations reflects the sum of electrophoretic and electroosmotic coupling at the bilayer interface. If the receptor is weakly charged, electroosmotic effects will dominate. This was manifested in the MHC transport experiments where the MHC receptors electromigrated toward the cathode.

Rectification mechanism

The mechanism of cell shape–dependent rectification of receptor distribution demonstrated by this model appears to be related to receptor mutual diffusion rates. Different cell geometries excite modes of mutual diffusion that differ significantly in time constants. The importance of surface geometry can be appreciated by comparing the redistribution response in cells of two different shapes shown in Fig. 5. There exists a plane of symmetry normal to the axis of electromigration in Fig. 5 *a*, *left*, but not in Fig. 5 *a*, *right*. This difference in surface geometry caused the two profiles to differ markedly. Because the included angle at the pole denoted by the point *B* of the asymmetrical surface in Fig. 5 *a*, *right*, was larger than that at the comparable apex in Fig. 5 *a*, *left*, receptors at that pole in Fig. 5 *a*, *right*, experienced more rapid back-diffusion and less receptor accumulation than those at the comparable apex in Fig. 5 *a*, *left*. At the opposite pole, the more acute angle caused an increased accumulation of receptors. In contrast, the symmetrical geometry (Fig. 5 *a*, *left*) was characterized by equal back-diffusion time constants at the two ends, resulting in equal magnitudes of receptor displacement. This finding demonstrates that cell shape is an important determinant of the magnitude of receptor accumulation at regions of cell taper in response to applied sinusoidal electric fields.

Our simulations indicate that significant receptor accumulation is found at tapered ends of cells in an applied field. This rectification is characterized by a threshold field frequency requirement, above which there is no significant time-averaged receptor displacement. A higher value of receptor electromigration mobility or applied field strength results in a higher cutoff frequency. In a 10-V/cm sinusoidal field in the millihertz frequency range, receptors on a cell 40 μm in length must have a diffusion coefficient to electromigration mobility ratio of <2.0 mV to generate a significant level of accumulation.

We found good agreement between theory and experiment in studies involving receptor distribution on human fibroblasts. There are several possible reasons for the small discrepancy between the results obtained by experiment and simulation. These include cell to cell variation in receptor immobile fraction, the presence or absence of membrane microdomains, and the presence or absence of class I MHC protein interactions with other transmembrane or membrane skeletal proteins. For example, protein-rich domains of μm-scale diameter have been found in plasma membranes of many cell types, including fibroblasts and hepatoma cells (Yechiel and Edidin, 1987; Edidin, 1990). These domains may be organized by lipid phase separations or by intramembrane protein interactions. Such interactions can significantly constrain protein movement in the plane of the lipid bilayer (Benveniste et al., 1988; Ryan et al., 1988). The location, size, and number of membrane microdomains affect the diffusibility of proteins in the cell membrane. Since our simulations did not take the presence of domains into account, the difference in τ_-/τ_+ values obtained from experiment and simulation could have resulted from the presence of such domains.

Crowding effects

As previously demonstrated by Ryan et al. (1988) and Saxton (1987), intermolecular receptor interactions and receptor crowding appear to affect substantially the diffusibility of receptors at high density. We confirm here that the predictions of these simulations are consistent with the Fermi–Dirac equilibrium statistical model (Ryan et al., 1988).

In these studies, we assumed that receptors undergo back-diffusion to a uniform distribution after termina-

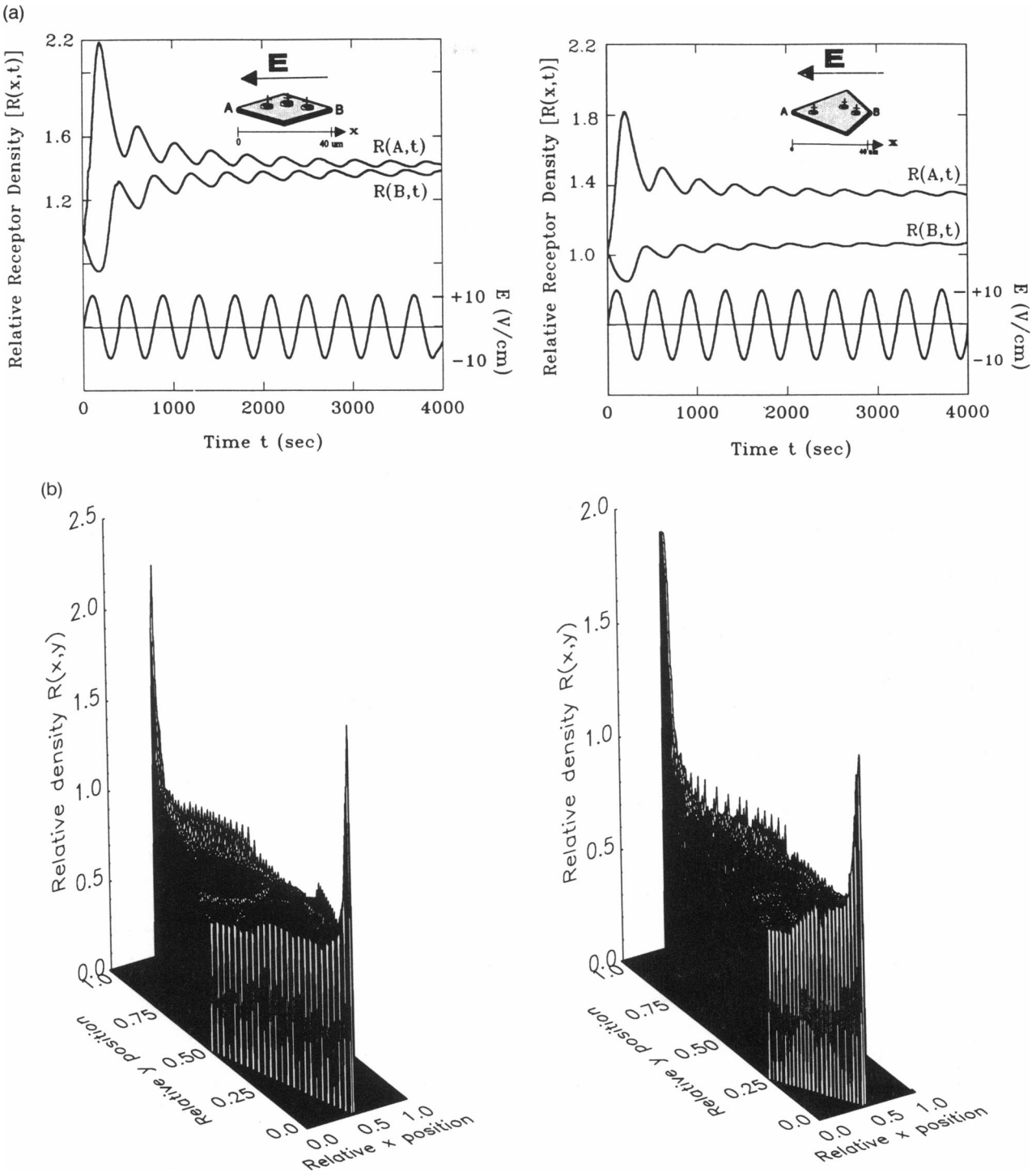

FIGURE 5 (*a*) Effect of asymmetry on normalized receptor density at two points (*A* and *B*) on a symmetrical (*left*) and an asymmetrical (*right*) rhomboid-shaped surface after the application of a 10-V/cm, 2.5-mHz sinusoidal field. Receptors have an effective electromigration mobility of 1.2×10^{-6} cm^2/V-s and a lateral diffusion coefficient of 2.3×10^{-9} cm^2/s. (*b*) Effect of cell shape on receptor transport. Equilibrium receptor distribution on an asymmetrical (*left*) and a asymmetrical (*right*) surface in a 10-V/cm sinusoidal field. The effect of cell shape on receptor transport rectification is reflected by the shift in the center of mass of the equilibrium distribution of receptors.

tion of the electric field. This assumption may not be valid in all cases, however. Acetylcholine receptors readily form immobile aggregates after electric field–induced receptor crowding (Young et al., 1984). Young et al. (1984) report that these aggregates remain localized at the cathodal pole of the cell for up to 2 d in culture. Poo (1981) observed that after the termination of the field, a small acetylcholine receptor cluster formed by

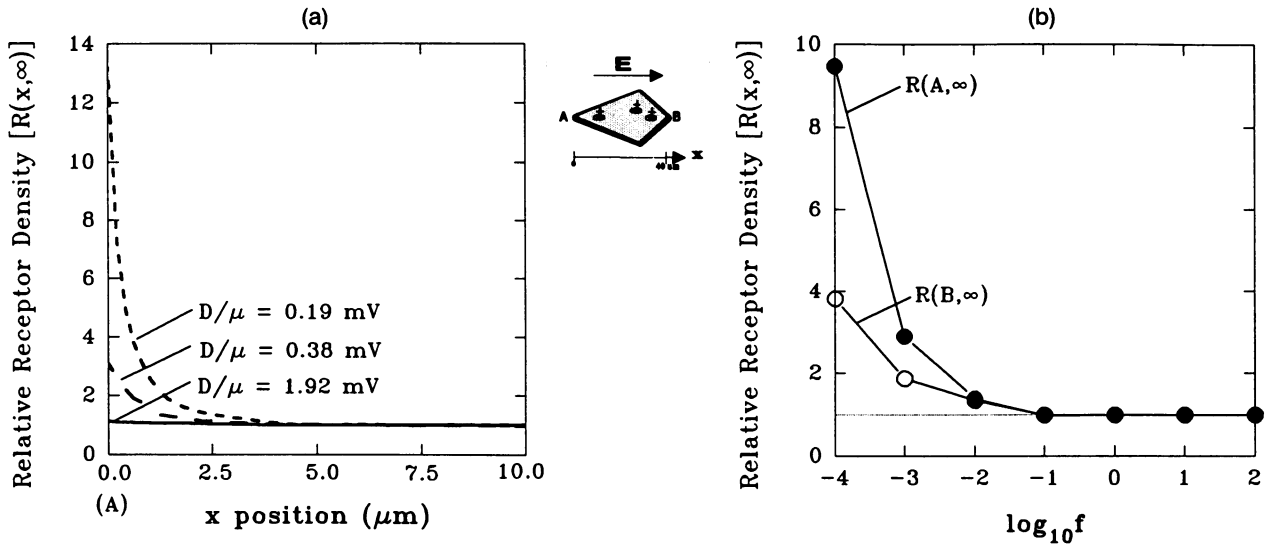

FIGURE 6 (*a*) Effect of electromigration mobility on receptor transport in a sinusoidal field. For a receptor with a lateral diffusion coefficient of 2.3×10^{-9} cm^2/s in an applied 0.1-Hz sinusoidal field of 20 V/cm, an order of magnitude change in electromigration mobility causes a large change in equilibrium receptor density at the narrow apex. (*b*) Effect of sinusoidal field frequency on rectification of receptor redistribution. Rectification of receptor transport behaves as a low-pass filter. The strength of the applied sinusoidal field was 10 V/cm, the receptor diffusion coefficient was 2.3×10^{-9} cm^2/s, and the electromigration mobility was 1.2×10^{-6} cm^2/V-s.

brief treatment with a dc field can increase in size and even form a large receptor cluster. Rectification of receptor transport in a sinusoidal field could induce the formation of similarly long-lived clusters on the cell surface.

Receptor redistribution could influence the kinetics of receptor-ligand interactions. Clustering of two or more receptors on the surface of cells is an important event in certain types of transmembrane signaling (Perelson, 1984). Histamine release from basophils or mast cells, for example, cannot be stimulated by monovalent ligands but can be induced by multivalent analogs capable of cross-linking receptors. Basophil desensitization also can be induced by receptor cross-linking. Receptor cross-linking can therefore generate both stimulatory and inhibitory signals; the cellular response of the basophil appears to depend on a balance between these signals (DeLisi and Siraganian, 1979; Chabay et al., 1980; Dembo and Goldstein, 1980). Similar phenomena have been observed with regard to the stimulation of B lym-

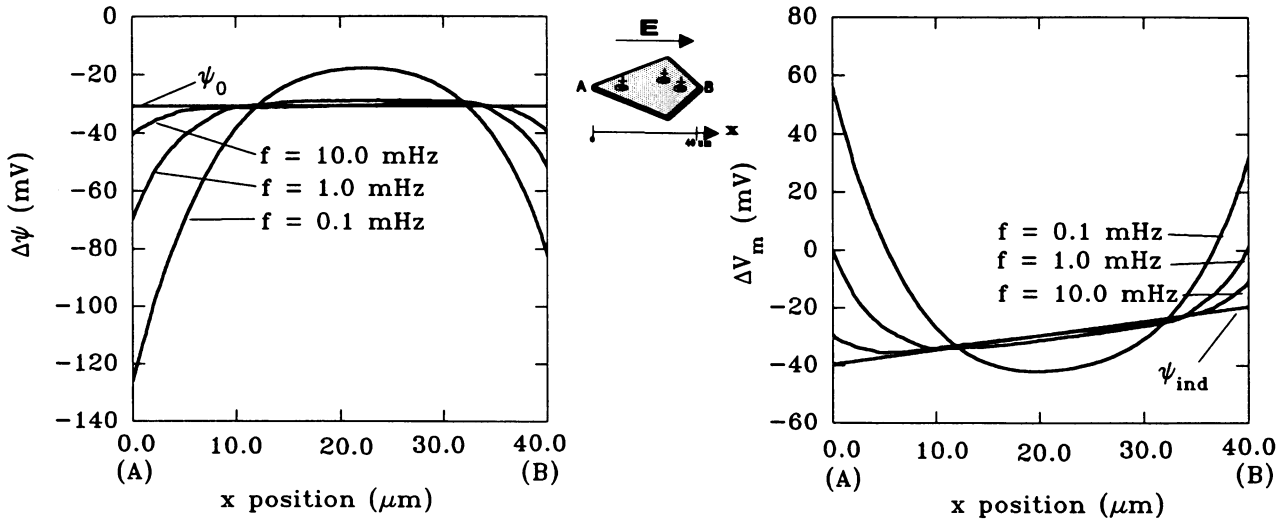

FIGURE 7 Time-average transmembrane potential distribution in a sinusoidal field. The change in transmembrane potential due to the redistribution of receptors $\Delta\psi$ (*left*) is greater than the change due to the direct effect of the applied field by an order of magnitude at very low frequencies. The transmembrane potential is also shown (*right*). The profiles shown are for receptors of electromigration mobility of 1.2×10^{-6} cm^2/V-s and diffusion coefficient of 2.3×10^{-9} cm^2/s in a 10-V/cm sinusoidal field.

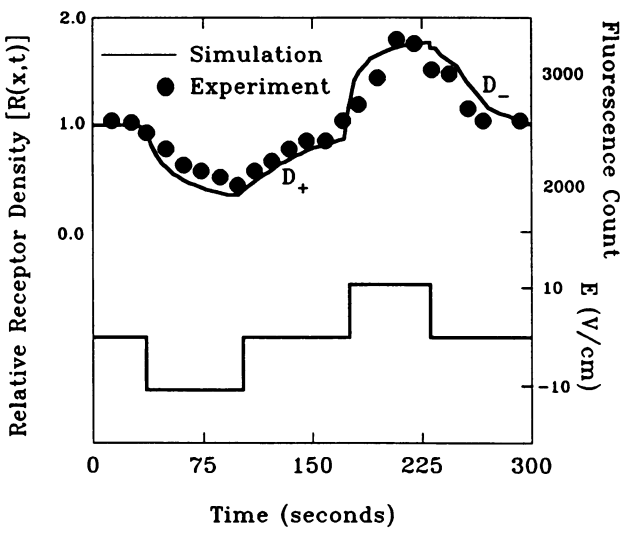

	τ_-	χ^2	τ_+	χ^2	τ_-/τ_+
1	54.4	0.03	36.5	0.05	1.49
2	75.0	0.40	97.9	0.16	0.77
3	26.3	0.11	11.7	0.07	2.24
4*	72.6	0.46	62.8	0.18	1.16
5	92.4	0.10	67.4	0.20	1.37
6	124.9	0.14	87.4	0.19	1.42
7*	11.1	0.47	13.6	0.31	0.82
8*	77.6	0.22	50.3	0.11	1.54
	$(\tau_-/\tau_+) = 1.35 \pm 0.46$ (s.d.)				

FIGURE 8 Comparison of simulation and experimental results. Concentration evolution of relative receptor density at the "*leading edge*" of a fibroblast cell predicted by the finite difference model (*solid line*) is compared with the experimental results (*filled circles*). The experimental back-diffusion characteristic times are shown in the table (*right*) with mean and standard deviation. Asterisks indicate experiments in which the negative field was applied first. The average ratio τ_-/τ_+ was found to be significantly different from 1.0 with a P value, by Student's two-tailed t test, of <0.025.

phocytes: multivalent ligands in the absence of T lymphocytes are effective in stimulating B cells, whereas monovalent ligands are ineffective. Dintzis et al. (1976) and Vogelstein et al. (1982) have hypothesized that a cluster of 10–20 receptors, an "immunon," is required to stimulate a B cell in the absence of T cells. Experiments by Dintzis et al. (1983) also indicate that cluster formation is a necessary step in the induction of B cell tolerance; receptor clusters that are too small to form an immunon lead not to stimulation but to immunologic tolerance. High levels of receptor aggregation due to rectification of transport under low-frequency sinusoidal fields could result in corresponding increases in receptor-ligand pairs. This change in the density of receptor-ligand pairs could promote patching, coated pit formation, or capping, which could in turn alter rates of endocytosis, exocytosis, or other ligand-controlled cellular responses.

Other cellular functions that are influenced by extracellular electric fields include the oriented migration of fibroblasts (Stump and Robinson, 1982), neural crest cells (Cooper and Keller, 1983), and growing neurite tips toward the pole of receptor aggregation (Hinkle et al., 1981; Patel and Poo, 1982). Migration of neurite surface con A receptors has been correlated with the neurite surface orientation response in the oriented growth of cultured *Xenopus* neurons.

Altered surface potential

Redistribution of charged cell surface receptors changes the transmembrane potential (McLaughlin, 1977). For sinusoidal fields of very low frequency and receptors of high mobility, our results suggest that the change in transmembrane potential distribution after receptor aggregation can be significantly greater than that due to the direct effect of the applied electric field. Peak changes in transmembrane potential depend on, among other factors, the mobile fraction of receptors on the cell. For example, con A receptors on *Xenopus* myotomal cells (Poo et al., 1979) have a mobile fraction of 0.5, whereas Fc receptors on rat basophilic leukemia cells have a mobile fraction of 0.7 (Ryan et al., 1988) to 0.85 (Menon et al., 1986; Thomas et al., 1992). For cells with a smaller fraction of mobile receptors, the magnitude of transmembrane potential change could be less than that shown here.

Many biological processes, such as oocyte and embryo development (Jaffe, 1979; Overall and Jaffe, 1985), tissue regeneration (Borgens et al., 1977, 1981; Jaffe and Poo, 1979), and tissue repair by artificial electrical stimulation (Bassett et al., 1964; Brighton and Pollack, 1984), may be influenced by altered transmembrane potential. Large deviations from steady-state potential distributions could influence the response of cells to endogenous currents or other membrane-related transduction events. For example, a large change in transmembrane potential generated by receptor redistribution could facilitate the repolarization of portions of the cell membrane that have relative aggregation of receptors.

SUMMARY AND CONCLUSION

The most important conclusion from this study is that rectification of receptor transport in a sinusoidal electric field can result from certain asymmetrical cell shapes. We define rectification as a shift in receptor center of

mass on the cell surface. Cell shape can therefore be an important deterministic factor in the cellular response to an extracellular sinusoidal electric field. If the cell has no plane of symmetry about the axis of receptor electromigration, then a shift in the center of mass of cell surface receptors can occur. This phenomenon results from the dependence of receptor mutual diffusion on cell surface geometry. Substantial alteration in transmembrane potential due to redistribution of cell surface receptors may also occur. Thus, important biological effects can be expected when nonspherical, asymmetrical cells that possess mobile cell surface receptors are exposed to very low frequency sinusoidal electric fields.

We thank Drs. James R. Melcher, Alan J. Grodzinsky, and Watt W. Webb for helpful comments and suggestions.

In addition, we acknowledge the support of the Whitaker Fund of The Massachusetts Institute of Technology (R. C. Lee and D. E. Golan), the Searle Scholars Program of The Chicago Community Trust (R. C. Lee, no. 85-B-106), and the National Institutes of Health (D. E. Golan, HL-32854).

Received for publication 16 March 1992 and in final form 2 September 1992.

REFERENCES

Barnstable, C. J., W. F. Bodmer, G. Brown, G. Galfre, C. Milstein, A. F. Williams, and A. Ziegler. 1978. Production of monoclonal antibodies to group A erythrocytes, HLA and other human cell surface antigens–new tools for genetic analysis. *Cell.* 14:9–20.

Basch, R. M. 1988. Evidence of anisotropic mechanical properties of fibroblast membranes. M.S. thesis. Massachusetts Institute of Technology, Cambridge, MA. 127 pp.

Bassett, C. A. L., R. J. Pawluk, and R. O. Becker. 1964. Effects of electric currents on bone in vivo. *Nature (Lond.).* 204:652–654.

Benveniste, M., E. Livneh, J. Schlessinger, and Z. Kam. 1988. Overexpression of epidermal growth factor receptor in NIH-3T3-transfected cells slows its lateral diffusion and rate of endocytosis. *J. Cell Biol.* 108:481–493.

Borgens, R. B., J. W. Vanable, Jr., and L. F. Jaffe. 1977. Bioelectricity and regeneration by minute currents. *J. Exp. Zool.* 200:403–416.

Borgens, R. B., E. Roederer, and M. J. Cohen. 1981. Enhanced spinal cord regeneration in lamprey by applied electric fields. *Science (Wash. DC).* 213:611–617.

Brighton, C. T., and S. R. Pollack. 1984. Treatment of nonunion of the tibia with a capacitatively coupled electric field. *J. Trauma.* 24:153–155.

Chabay, R., C. DeLisi, W. A. Hook, and R. P. Siraganian. 1980. Receptor cross-linking and histamine release in basophils. *J. Biol. Chem.* 255:4628–4635.

Cooper, M. S., and R. E. Keller. 1983. Perpendicular orientation and directional migration of amphibian neural crest cells in DC electrical fields. *Proc. Natl. Acad. Sci. USA.* 81:160–164.

DeLisi, C., and R. P. Siraganian. 1979. Receptor cross-linking and histamine release. II. Interpretation and analysis of anomalous dose response patterns. *J. Immunol.* 122:2293–2299.

Dembo, M., and B. Goldstein. 1980. A model of cell activation and desensitization by surface immuno-globulin: the case of histamine release from human basophils. *Cell.* 22:59–67.

Dintzis, H. M., R. Dintzis, and B. Vogelstein. 1976. Molecular determinants of immunogenicity: the immunon model of immune response. *Proc. Natl. Acad. Sci. USA.* 73:3671–3675.

Dintzis, R. Z., M. H. Middleton, and H. M. Dintzis. 1983. Studies on the immunogenicity and tolerogenicity of T-independent antigens. *J. Immunol.* 131:2196–2203.

Edidin, M. 1990. Molecular associations and membrane domains. *Curr. Top. Membr. Transp.* 36:81–96.

Edidin, M., and T. Wei. 1982. Lateral diffusion of H-2 antigens on mouse fibroblasts. *J. Cell Biol.* 95:458–462.

Eisinger, J., and B. I. Halperin. 1986. Effects of spatial variation in membrane diffusibility and solubility on the lateral transport of membrane components. *Biophys. J.* 50:513–521.

Golan, D. E., M. R. Alecio, W. R. Veatch, and R. R. Rando. 1984. Lateral mobility of phospholipid and cholesterol in the human erythrocyte membrane: effects of protein-lipid interactions. *Biochemistry.* 23:332–339.

Golan, D. E., C. S. Brown, C. M. L. Cianci, S. T. Furlong, and J. P. Caulfield. 1986. Schistosomula of *Schistosoma mansoni* use lysophosphatidylcholine to lyse adherent human red blood cells and immobilize red cell membrane components. *J. Cell Biol.* 103:819–828.

Goodman, R., C. A. L. Bassett, and A. S. Henderson. 1983. Pulsing electromagnetic fields induce cellular transcription. *Science (Wash. DC).* 220:1283–1285.

Gross, D. 1988. Electromobile surface charge alters membrane potential changes induced by applied electric fields. *Biophys. J.* 54:879–884.

Gross, D., W. S. Williams, and J. A. Connor. 1983. Theory of electromechanical effects in nerve. *Cell. Mol. Neurobiol.* 3:89–111.

Gross, D., L. M. Loew, and W. W. Webb. 1986. Optical imaging of cell membrane potential changes induced by applied electric fields. *Biophys. J.* 50:339–348.

Guigni, T. D., D. L. Braslau, and H. T. Haigler. 1987. Electric field-induced redistribution and postfield relaxation of epidermal growth factor receptors on A431 cells. *J. Cell Biol.* 104:1291–1297.

Hildebrand, F. B. 1968. *Finite-Difference Equations and Simulations.* Prentice-Hall, Englewood Cliffs, NJ. 338 pp.

Hinkle, L., C. D. McCaig, and K. R. Robinson. 1981. The direction of growth of differentiating neurons and myoblasts from frog embryos in an applied electric field. *J. Physiol. (Lond.).* 314:121–135.

Jaffe, L. F. 1979. Control of development by ionic currents. *In* Membrane Transduction Mechanisms. R. A. Cone and J. E. Downing, editors. Raven Press, New York. 199–231.

Jaffe, L. F., and R. Nuccitelli. 1977. Electrical controls of development. *Annu. Rev. Biophys. Bioeng.* 10:245–276.

Jaffe, L. F., and M.-m. Poo. 1979. Neurites grow faster towards the cathode than the anode in a steady field. *J. Exp. Zool.* 209:115–128.

Lauffer, M. A. 1989. *Motion in Biological Systems.* Alan R. Liss, Inc. New York. 259 pp.

McCloskey, M. A., Z.-Y. Liu, and M.-m. Poo. 1984. Lateral electromigration and diffusion of Fc receptors on rat basophilic leukemic cells: effects of IgE binding. *J. Cell Biol.* 99:778–787.

McLaughlin, S. 1977. Electrostatic potentials at membrane-solution interfaces. *Curr. Top. Membr. Transp.* 9:71–144.

McLaughlin, S., and M.-m. Poo. 1981. The role of electro-osmosis in the electric field-induced movement of charged macromolecules on the surface of cells. *Biophys. J.* 34:85–93.

McLeod, K. J., R. C. Lee, and H. P. Ehrlich. 1987. Frequency dependence of electric field modulation of fibroblast protein synthesis. *Science (Wash. DC).* 236:1465–1469.

Menon, A. K., D. Holowka, W. W. Webb, and B. Baird. 1986. Clustering, mobility, and triggering activity of small oligomers of immunoglobulin E on rat basophilic leukemia cells. *J. Cell Biol.* 102:534–540.

Overall, R., and L. F. Jaffe. 1985. Patterns of ionic current through *Drosophila* follicles and eggs. *Dev. Biol.* 108:102–119.

Patel, N. B., and M.-m. Poo. 1982. Orientation of neurite growth by extracellular electric fields. *J. Neurosci.* 2:483–496.

Perelson, A. S. 1984. Some mathematical models of receptor clustering by multivalent ligands. *In* Cell Surface Dynamics: Concepts and Models. A. S. Perelson, C. DeLisi, and F. W. Wiegel, editors. Marcel Dekker, Inc., New York. 223–276.

Peters, R., and R. J. Cherry. 1982. Lateral and rotational diffusion of bacteriorhodopsin in lipid bilayers: experimental test of the Saffman-Delbrück equations. *Proc. Natl. Acad. Sci. USA.* 79:4317–4321.

Pink, D. A., D. J. Laidlaw, and D. M. Chisholm. 1986. Protein lateral movement in lipid bilayers. Monte Carlo simulation studies of its dependence upon attractive protein-protein interactions. *Biochim. Biophys. Acta.* 863:9–17.

Poo, M.-m. 1981. In situ electrophoresis of membrane components. *Annu. Rev. Biophys. Bioeng.* 10:245–276.

Poo, M.-m., and K. R. Robinson. 1977. Electrophoresis of concanavalin A receptors along embryonic muscle cell membrane. *Nature (Lond.).* 265:602–605.

Poo, M.-m., J. W. Lam, N. Orida, and A. W. Chao. 1979. Electrophoresis and diffusion in the plane of the cell membrane. *Biophys. J.* 26:1–22.

Press, W. H., B. P. Flannery, S. A. Twukolsky, and W. T. Vetterling. 1986. *Numerical Recipes. The Art of Scientific Computing.* Cambridge University Press, Cambridge, U.K. 759 pp.

Ryan, T. A., J. Myers, D. Holowka, B. Baird, and W. W. Webb. 1988. Molecular crowding on the cell surface. *Science (Wash. DC).* 239:61–64.

Saffman, P. G., and M. Delbrück. 1975. Brownian motion in biological membranes. *Proc. Natl. Acad. Sci. USA.* 72:3111–3113.

Saxton, M. J. 1982. Lateral diffusion in an archipelago: effects of impermeable patches on diffusion in a cell membrane. *Biophys. J.* 39:165–173.

Saxton, M. J. 1987. Lateral diffusion in an archipelago: the effect of mobile obstacles. *Biophys. J.* 52:989–997.

Schlessinger, J., Y. Schechter, M. C. Willingham, and I. Pastan. 1978. Direct visualization of binding, aggregation, and internalization of insulin and epidermal growth factor on living fibroblastic cells. *Proc. Natl. Acad. Sci. USA.* 75:2659–2663.

Smith, B. A., W. R. Clark, and H. M. McConnell. 1979. Anisotropic molecular motion on cell surfaces. *Proc. Natl. Acad. Sci. USA.* 76:5641–5644.

Stolpen, A. H., J. S. Pober, C. S. Brown, and D. E. Golan. 1988. Class I major histocompatibility complex proteins diffuse isotropically on immune interferon-activated endothelial cells despite anisotropic cell shape and cytoskeletal organization: application of fluorescence photobleaching recovery with an elliptical beam. *Proc. Natl. Acad. Sci. USA.* 85:1844–1848.

Stump, R. F., and K. R. Robinson. 1982. Directed movements of *Xenopus* embryonic cells in an electric field. *J. Cell Biol.* 95:331*a*. (Abstr.)

Tank, D. W., E.-S. Wu, and W. W. Webb. 1982. Enhanced molecular diffusibility in muscle membrane blebs: Release of lateral constraints. *J. Cell Biol.* 92:207–212.

Thomas, J. L., T. J. Feder, and W. W. Webb. 1992. Effects of protein concentration on IgE receptor mobility in rat basophilic leukemia cell plasma membranes. *Biophys. J.* 61:1402–1412.

Vaz, W. L. C., F. Goodsaid-Zalduondo, and K. A. Jacobson. 1984. Lateral diffusion of lipids and proteins in bilayer membranes. *FEBS (Fed. Eur. Biochem. Soc.) Lett.* 174:199–207.

Vogelstein, B., R. Z. Dintzis, and H. M. Dintzis. 1982. Specific cellular stimulation in the primary immune response: a quantized model. *Proc. Natl. Acad. Sci. USA.* 79:395–399.

Weaver, J. C., and R. D. Astumian. 1990. The response of living cells to very weak electric fields: the thermal noise limit. *Science (Wash. DC).* 247:459–462.

Wolf, D. E., M. Edidin, and P. R. Dragsten. 1980. Effect of bleaching light on measurements of lateral diffusion in cell membranes by the fluorescence photobleaching recovery method. *Proc. Natl. Acad. Sci. USA.* 77:2034–2045.

Yechiel, E., and M. Edidin. 1987. Micrometer-scale domains in fibroblast plasma membranes. *J. Cell Biol.* 105:755–760.

Young, S. H., M. McCloskey, and M.-m. Poo. 1984. Migration of cell surface receptors induced by extracellular electric fields: theory and applications. *In* The Receptors. Vol. I. P. M. Conn, editor. Academic Press, New York. 511–539.

Zimmermann, U. 1982. Electric field-mediated fusion and related electrical phenomena. *Biochim. Biophys. Acta.* 694:227–277.